CLINICAL APPLICATIONS OF A KINETIC MODEL OF HIPPURATE DISTRIBUTION AND RENAL CLEARANCE

Joseph A. DeGrazia, Paul O. Scheibe, Peter E. Jackson, Zoltan J. Lucas, William R. Fair, John M. Vogel*, and Leonard J. Blumin

Stanford Medical Center, Stanford, California, Analytical Development Associates Corporation, Cupertino, California, Community Hospital of Los Gatos-Saratoga, Los Gatos, California, USPHS Hospital, San Francisco, California, and Veterans Administration Hospital, San Francisco, California

Measurements of effective renal plasma flow and urine flow fractions have been obtained by the application of a new kinetic model of o-iodohippurate distribution and renal clearance. Good agreement was obtained between these estimates and those of comparable parameters obtained by conventional split-function techniques using p-aminohippurate and inulin. Also, examples have been presented of the use of this test for the evaluation of patients suffering from well-documented renal diseases. These uses have included serial testing in patients with major renal artery occlusion, bilateral renal vein thrombosis, obstruction due to stone, or transplant rejection. It was concluded that this test can be of considerable value for the diagnosis of acute and chronic disorders of renal function and for evaluation of the therapeutic response. In addition, these studies have demonstrated the potential of large computers for parameter estimation in the interpretation of nuclear medicine procedures.

The radiohippurate renogram is a time-dependent composite presentation of isotope turnover in blood, renal, and extrarenal tissues. Unfortunately, the clinical evaluation of this test in the past has been both subjective and qualitative since there has been no determination of the relative contribution of the exchanges in each of these tissues to the final result (*1–4*). Consequently, the renogram does not have desired diagnostic precision. As a result, investigators have sought to improve it by developing more objective criteria for its interpretation (*5–9*). In general, these newer techniques have not gained widespread use since, like the renogram, they still do not yield the basic parameters of renal physiology of interest to the clinician.

Recent advances in nuclear medicine instrumentation and computing have made it possible to further develop the radiohippurate method so that it is a quantitative measure of specific kidney functions (*10–15*). In general, these methods have used a computer to aid in the adjustment of the variable parameters of a mathematical description of hippurate turnover in the body to extract quantitative clinically useful data not usually obtained from the conventional renogram.

In this paper we report the first clinical application of a new split-function renal test using an extension of earlier approaches (*14–16*). The model used is a hydraulic analog that considers the distribution and rates of exchange of isotope into red cells, plasma, and extravascular compartments as well as the tubular cells of each kidney. Also included is the clearance of isotope from the tubular cells and the transport time of isotope in urine to the bladder. The results obtained are very similar to those obtained in conventional split-function renal testing using *p*-aminohippurate (PAH) and inulin (*17*). The results are thus familiar to the physician interested in renal diseases. The new test is not invasive and is easy to perform. To avoid confusion with the ordinary renogram, we have named this test the "renal perfusion/excretion determination" (RP/ED).

Received Feb. 15, 1973; revision accepted Sept. 6, 1973.

For reprints contact: Joseph A. DeGrazia, Div. of Nuclear Medicine, Stanford Medical Center, Stanford, Calif. 94305.

* Present address: Department of Radiology, School of Medicine, University of California, Davis, California 95616.

METHODS

Selection of patients. Eighty studies were performed on a total of 49 patients. Included are: 25 normal subjects; 14 patients in whom renal transplants had been performed; 6 patients with surgically confirmed unilateral, main renal artery occlusion; 1 patient with essential hypertension; 1 patient each with renal vein thrombosis, urinary obstruction due to stones, and hydronephrosis. The diagnoses of renal vein thrombosis and hydronephrosis were confirmed surgically. A hydroxyapatite stone was recovered in the patient with urinary obstruction. Renal transplant patients were additionally studied with serial measurements of creatinine clearance, 24-hr urine flow, and, when clinically indicated, a renal biopsy.

RP/ED procedure. Ambulatory patients were studied in a specially designed chair that permitted them to recline against the face of the gamma camera at an angle of 45 deg. The patient was given 500 μCi of ^{99m}Tc-DTPA (RENOTEC®) and was then positioned so that one kidney was located in each field of the gamma camera (operated in the split-field mode). Effort was made to reduce the amount of bladder in the field of view although some contribution (usually less than 5%) was felt to be acceptable. An additional probe was then placed over the precordium while another was placed over the entire bladder. Care was taken to avoid viewing the kidney with these probes. Next, 300 μCi of ^{131}I-orthoiodohippurate (OIH) was given intravenously. Data from each of the four detectors was then recorded at 10-sec intervals for 5 min and at 30-sec intervals thereafter using a teletypewriter with paper tape punch. Transplant patients were studied with the gamma camera directly over the abdomen so that the transplant kidney was positioned in the first half of the gamma camera field and the bladder in the second. A probe was then placed over the precordium. Gamma camera scintiphotos were also obtained during localization with ^{99m}Tc-DTPA and at 3- to 5-min intervals after injection of OIH.

Patient preparation included adjustment of water intake when necessary to achieve a steady state of normal hydration and a urine flow rate of 0.5–3 ml/min. Also, Lugol's solution (5–10 drops) was given to reduce thyroid gland uptake of free iodine. Whenever possible, the plasma volume was measured with 10 μCi of ^{125}I-albumin using blood samples obtained at 10- and 20-min intervals. Timed total urine flow during the study was also recorded. When the study was completed, the data were transmitted to an S-R Univac 1108 computer for processing. Results were returned to the medical facility by teletypewriter in the format shown in Fig. 1.

```
*** MEDNET ***

RENAL PERFUSION/EXCRETION DETERMINATION

FOR: STANFORD UNIVERSITY HOSPITAL                    PRIORITY: ROUTINE

REFERRING PHYSICIAN: JACKSON                          DATE: 4-5-72

PATIENT: DOE, ROSE

   AGE: 45      SEX: FEMALE     ID: 01-925

                                    RESULTS   STANDARD ERROR        NORMAL RANGE

PRIMARY DETERMINATIONS:
------- --------------

  RENAL PERFUSION                   0.2300    0.0081 ( 3.5%)      .13-.31
  COEFFICIENT (PER MIN)

  BILATERAL PERFUSION    LEFT       0.5089    0.0262 ( 5.1%)      .42-.58
  FRACTION               RIGHT      0.4911    0.0262 ( 5.3%)      .42-.58

  TUBULAR CELL CLEARANCE LEFT       0.3118    0.0174 ( 5.6%)      .15-1.0
  COEFFICIENT (PER MIN)  RIGHT      0.2934    0.0168 ( 5.7%)      .15-1.0

  TUBULAR TRANSPORT      LEFT       2.1091    0.2600 (12.3%)      1.0-5.0
  TIME (IN MINUTES)      RIGHT      2.0465    0.2884 (14.1%)      1.0-5.0

DERIVED RESULTS:
------- -------

  UNILATERAL PERFUSION   LEFT       0.1171    0.0072 ( 6.2%)      .06-.16
  COEFFICIENT (PER MIN)  RIGHT      0.1129    0.0073 ( 6.5%)      .06-.16

  URINE FLOW             LEFT       0.5014    0.0710 (14.2%)      .36-.64
  FRACTION               RIGHT      0.4986    0.0710 (14.2%)      .36-.64

  OIH CONC. RATIO        (R/L)      0.9703    0.1796 (18.5%)      .67-1.0

COMMENT:
      A GOOD FIT TO THE FOUR DATA CHANNELS (LEFT, RIGHT KIDNEY
      BLADDER, AND PRECORDIAL).

*** MEDNET ***
```

FIG. 1. RP/ED report: Includes estimates for each parameter, standard error, and normal (95%) parameter range. Report is augmented to include description of scintiphotos when sent to referring physician.

COMPUTATIONS

Physiological assumptions. Following injection, OIH is distributed between free OIH in plasma, the red cells, plasma proteins, as well as interstitial and extracellular spaces (*18–21*). Exchange between the free and bound state in plasma and the extravascular spaces is rapid (*22,23*). Glomerular flow of OIH is small (~6% of tubular cell plasma clearance) (*19,20*). Once in the kidney, OIH is actively pumped into the proximal tubular cells creating an interstitial concentration gradient that promotes flow out of the plasma and across the interstitial space (*24–26*). Nearly the entire plasma flow of OIH is cleared before it is efferent to the proximal tubular cells. OIH then diffuses passively from the tubular cells into the collecting system and is not reabsorbed.

The hydraulic model. A seven-compartment hydraulic model incorporating the features discussed above is shown in Fig. 2; a mathematical description is provided in the Appendix. The model also accounts for the fact that appreciable OIH has been deposited in extraplasma pools at the time that intrapool mixing has been accomplished (40–100 sec postinjection). Flow rates are everywhere assumed to be proportional to the quantity of tracer

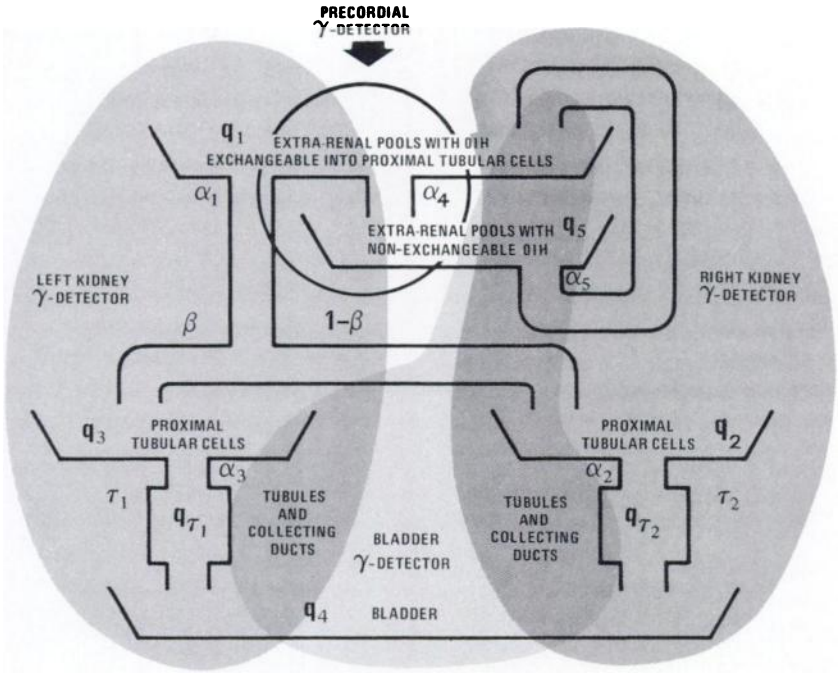

FIG. 2. Diagrammatic presentation of relationship of regions seen by four gamma detectors to compartments described by mathematical model. Shaded areas represent four gamma detector viewing fields.

material in the anatomic pool (*27*). Each flow rate between compartments is thus described by a constant rate coefficient (α) multiplied by a quantity of material (q) contained in any one of the compartments used in the model. The first compartment represents the extrarenal pools that participate in OIH exchange from the vascular system into proximal tubular cells. Practically, this compartment represents the plasma pool since there is limited availability of OIH from extravascular, interstitial, or extracellular spaces. Two coefficients (α_1 and α_4) describe the rate at which q_1 in Compartment 1 empties into other related compartments. The first of these, α_1, is the plasma clearance of OIH into the right and left proximal tubular cells (Compartments 2 and 3, respectively). α_1 is called the bilateral renal perfusion coefficient (RPC) on the RP/ED report. When α_1 is multiplied by the plasma volume, the volume of plasma completely cleared of OIH in 1 min is obtained. Although this product is more accurately viewed as a measure of the efficiency of tubular cell function, it is commonly called the effective renal plasma flow rate (ERPF) in split-function tests. This name reflects the fact that OIH uptake is normally primarily limited by blood flow to the tubular cells rather than by the very efficient OIH transport process (*25*). The values of β and $1-\beta$ are are the fraction of isotope flow in blood to the left and right kidneys, respectively. These are reported as the left and right bilateral perfusion fraction in the RP/ED report. α_2 and α_3 are the rate coefficients for the flow of OIH from the tubular cells into the tubular lumen of the right and left kidney, respectively. They are called the tubular cell clearance coefficient (TCCC) on the RP/ED report. α_2 and α_3 will increase as GFR, cell permeability, or intracellular osmolarity increases (and conversely) (*28*).

Once OIH enters the tubule and collecting system, it is assumed that it is carried to the bladder by laminar flow with little mixing (*29*)*. Consequently, the collecting duct outflow is simply a delayed replica of the tubular cell outflow as well as an inflow into the bladder compartment (Compartment 4). The time delay (τ_1 and τ_2) between tubular cell outflow and renal pelvic outflow is reported as tubular transport time (TTT) on the RP/ED report. Fluid flow in the collecting system is dependent upon the degree of hydration and varies from 0.5 to 15% of glomerular filtration rate. Since OIH is not reabsorbed, most of its TTT is spent in the distal collecting system of the kidney along with nonreabsorbed water. Variation in water reabsorption will thus significantly influence isotope transport through the collecting system; the TTT will be directly related to changes in water reabsorption for each kidney and inversely related to changes in the urine flow rate.

If it is also assumed that the effective number of

* The length-to-radius ratio of the tubular lumen is large (about 10,000), and flow is slow with a maximum Reynold's number of less than unity.

functioning nephrons in each kidney is proportional to the ERPF, it is possible to estimate the fraction of total urine flow produced by each kidney. The values of TTT can also be directly related to the urine OIH concentration ratio for each kidney (*10,28,30*). The urine flow fraction and urine OIH concentration ratio are reported on the RP/ED report as shown in Fig. 1. These are calculated as follows:

With β_L = fraction of total ERPF, left kidney
β_R = fraction of total ERPF, right kidney
τ_L = left TTT
τ_R = right TTT

Total urine flow, left kidney $\sim (\beta_L) \times (1/\tau_L)$
Total urine flow, right kidney $\sim (\beta_R) \times (1/\tau_R)$.

Hence, the fraction of total urine flow for the left kidney may be determined by

$$\frac{\beta_L/\tau_L}{\frac{\beta_L}{\tau_L}+\frac{\beta_R}{\tau_R}} \text{ or } \frac{\beta_L\tau_R}{\beta_L\tau_R+\beta_R\tau_L}.$$

Similarly, the right renal flow fraction is

$$\frac{\beta_R\tau_L}{\beta_L\tau_R+\beta_R\tau_L}.$$

The urine OIH concentration ratio is derived from the equation

$$\frac{\text{Left OIH concentration}}{\text{Right OIH concentration}}=\frac{\tau_L}{\tau_R}.$$

Not all of the OIH flowing through the kidney is extracted. Some is retained mainly in red cells. This pool is represented by the fifth model compartment of the RP/ED. α_4 and α_5 are the coefficients for flow of isotope into and out of this compartment, respectively. These coefficients are determined but not reported. Values of α_4 and α_5 from our studies of normal patients are in agreement with measurements by others (*18*).

Finally, full account is made of the cross-coupling between the fields of the gamma camera and the fact that different combinations of compartments are seen by the detectors.

Error analysis. Each RP/ED output form (Fig. 1) has a column labeled "standard error" that gives the square root of variance of each parameter. This error is determined by standard covariance calculations (*31*) described in the Appendix. The coefficient of variation (standard error divided by the parameter value), expressed as a percent, is also included in this column. The errors result primarily from statistical fluctuations in counting rate during the data collection process.

Normal ranges and RP/ED relationships to constant-infusion tests. Several measurements are theoretically common to both the RP/ED and to constant-infusion studies of PAH and inulin clearance [Stamey-Howard test (*32*)]. They are compared in Table 1. Since our series of patients is so small, normal RP/ED ranges have been derived from reports of constant-infusion tests (*17,32–38*). These include: 0.13–0.31 per minute for the RPC (*34,35*), 0.42–0.58 for the bilateral perfusion fraction (*17,36–38*), and 0.36–0.64 for the urine flow fraction (*37*). The normal TTT is estimated to range from 1 to 5 min, using published values for the size, number of tubules, reabsorption scheme of the tubules, and normal urine flow rates (*39,40*). Since the TCCC has no published counterpart, normal ranges are determined from RP/ED studies in our series. These

TABLE 1. RP/ED CORRESPONDENCE WITH CONSTANT-INFUSION SPLIT-FUNCTION MEASUREMENTS

Parameters obtained by the RP/ED	Parameters obtained by the constant-infusion test
For total function	
Renal perfusion coefficient	Total PAH clearance (ERPF) ÷ Plasma volume
$\frac{\text{Left tubular transport time}}{\text{Right tubular transport time}}$ = OIH urine concentration ratio (L/R)	Left urine PAH concentration ÷ Right urine PAH concentration
$\frac{\text{Left tubular cell clearance coefficient}^*}{\text{Right tubular cell clearance coefficient}}$	$\frac{\text{Left glomerular filtration fraction}}{\text{Right glomerular filtration fraction}}$
For each kidney	
Perfusion fractions	$\frac{\text{PAH clearance for one kidney}}{\text{Total PAH clearance}}$
Urine flow fractions	$\frac{\text{Urine flow rate for one kidney}}{\text{Total urine flow rate}}$

* Requires additional assumptions of similar OIH tubular cell permeabilities and osmolarity gradients in both kidneys to have equality of expressions in the two columns.

ranges appear in the last column of each RP/ED output form (Fig. 1).

The hypotheses presented above were tested by comparing estimates of renal function obtained by RP/ED and by constant-infusion studies with PAH and/or inulin in a small series of subjects. These include five uneventful, complete split-function tests by the method of Stamey, four tests in which only flow fractions and concentration ratios were obtained*, one test in which only urine flow fraction (creatinine split-function) was obtained, and three tests with only measurements of total PAH clearance (bladder catheter only). These are reported in the results section below.

RESULTS

Normal range and duplicate variation. The ranges for a series of 25 normal subjects have been determined. The mean values and standard deviation for this series are as follows: renal perfusion coefficient (RPC) is 0.22 ± 0.04, left bilateral perfusion fraction is 0.52 ± 0.08, tubular cell clearance coefficient (TCCC) is 0.44 ± 0.21, tubular transport time (TTT) is 2.3 ± 1.0, and urine flow fraction is 0.51 ± 0.11. The results of paired tests of control subjects in patients whose clinical status remained constant during the observation period appear in Table 2. In each of these series of studies the variation in test results is narrower for determination of parameters reflecting perfusion than it is for those measuring urine outflow. This dispersion is smallest for those patients with a measured urine flow rate between 0.5 and 2 ml/min (urine flow fraction was 0.50 ± 0.08 for flow rates between 0.5 and 2 ml/min).

Correlation with constant-infusion test results. Renal plasma flow fractions and urine flow fractions obtained by the RP/ED are compared in Fig. 3 to the fractions obtained by PAH constant-infusion tests with bilateral catheterization. Urine concentration ratios by both methods are compared in Fig. 4. The ERPF determinations are compared with PAH clearances in Fig. 5. A linear regression was done for each set of parameters; the sample correlation coefficient, ρ, is greater than 0.92 for the comparison of flow fractions, ρ is greater than 0.91 for comparison of PAH concentration ratios, and ρ is greater than 0.91 for the comparison of the total ERPF.

* Values of plasma PAH concentration approaching the tubular maximum (27) were obtained in these four tests; concentrations from 4.6 to 11.8 mg/100 ml were reported. Since these high concentrations may alter the total clearance (*41*), the only total clearance data we have used is from the remaining tests. The remaining PAH tests, of which all were used for total clearance, had plasma PAH concentrations less than 2.5 mg/100 ml with laboratory chemistry done as suggested by Stamey (*42*).

TABLE 2. A COMPARISON OF DUPLICATE RP/ED RESULTS IN CLINICALLY STABLE PATIENTS*

	RH		JV		CP		RB		DA	
	3/22/72	4/14/72	8/21/72	8/23/72	8/11/72	8/15/72	10/13/72	10/20/72	3/29/72	3/31/72
Renal perfusion coefficient (per min)	0.24 (±0.02)	0.230 (±0.008)	0.18 (±0.02)	0.127 (±0.004)	0.073 (±0.006)	0.093 (±0.007)	0.129 (±0.007)	0.144 (±0.008)	0.373 (±0.012)	0.37 (±0.02)
Bilateral perfusion coefficient (left)	0.53 (±0.03)	0.51 (±0.03)	0.44 (±0.04)	0.44 (±0.02)	0.314 (±0.013)	0.33 (±0.02)	0.27 (±0.05)	0.35 (±0.10)	Not applicable	
Tubular cell clearance coefficient (per min) (left)	1.5 (±0.4)	0.32 (±0.14)	0.74 (±0.13)	1.03 (±0.14)	0.022 (±0.007)	0.030 (±0.004)	<0.03	<0.03	0.06 (±0.02)	0.06 (±0.02)
Tubular transport time (left) (min)	2.21 (±0.12)	2.1 (±0.3)	1.4 (±0.3)	3.01 (±0.13)	14.0 (±4.0)	9.7 (±0.8)	>18	>20	3.2 (±0.8)	0.4 (±4.9)
Urine flow fraction (left)	0.40 (±0.04)	0.50 (±0.07)	0.50 (±0.09)	0.45 (±0.02)	0.25 (±0.06)	0.13 (±0.01)	<0.08	<0.06	Not applicable	
Clinical status	Normal		Normal		Left pyelonephritis		Left ureter obstructed		Stable transplant	
RP/ED conclusion	Normal		Normal		Low left ERPF & urine flow fraction		Reduced left ERPF left side obstruction		Acute rejection	

* Only the left values of bilateral determinations are given for brevity and clarity. Similar agreement is noted with the right values.

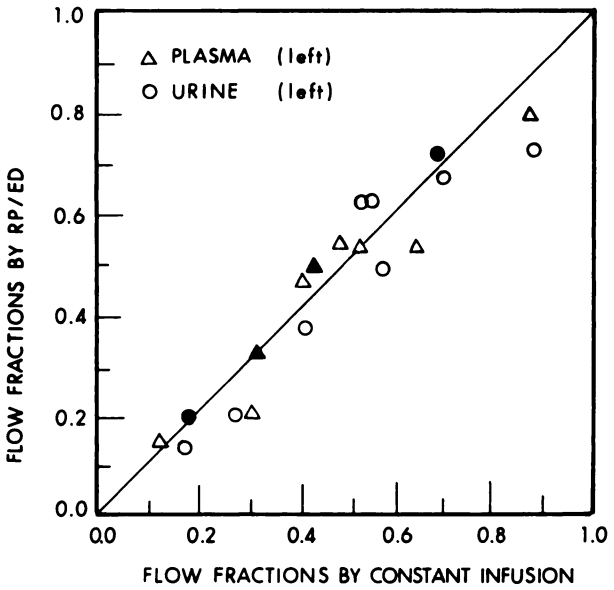

FIG. 3. Comparisons of renal plasma flow fractions and urine flow fractions obtained by RP/ED and constant-infusion split-function tests. Diagonal line is identity for reference. Darkened symbols represent cases of surgically proven unilateral main renal artery disease.

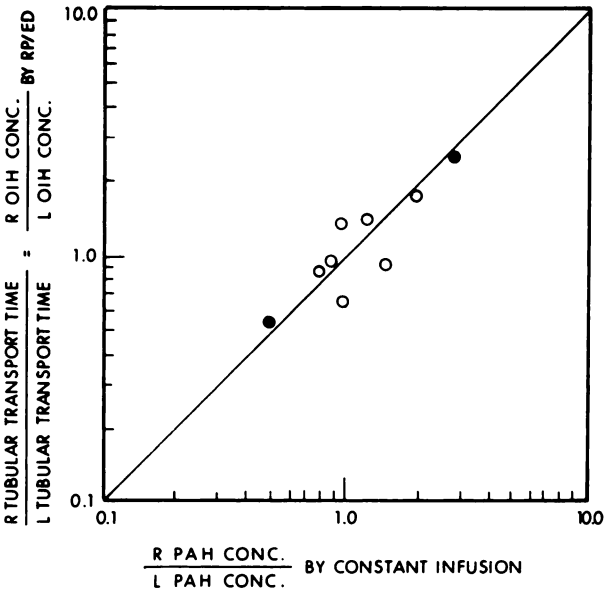

FIG. 4. Comparisons of urine concentration ratios, obtained by RP/ED and constant-infusion split-function tests. Diagonal line is identity for reference. Darkened symbols represent cases of surgically proven unilateral main renal artery disease.

Thus there is a high degree of correlation between these measurements even though they are obtained by different methods.

Clinical applications. The RP/ED has been used to evaluate differential function in a small series of patients with well-documented abnormalities of the kidney. These include renal vascular hypertension, obstruction due to stones, acute renal vein thrombosis, and rejection of the transplanted kidney. Selected cases are presented to show possible clinical applications and to illustrate the sensitivity of this test for the evaluation of the response to therapy or progress of renal disease.

Renal hypertension. Six patients with surgically proven unilateral major renal artery stenosis have been studied. Of these, six (100%) had an abnormal RP/ED that was characterized by a decrease in ischemic-to-contralateral ratio of ERPF (range is 0.30–0.97). Each had delayed TTT on the ischemic side; the ischemic-to-contralateral urine OIH concentration ratio was elevated (range 1.8–7.2) and the ischemic-to-contralateral urine flow ratio was reduced (range 0.05–0.39).

Serial studies (Fig. 6) of one patient (AM) demonstrates the reproducibility of this determination and its sensitivity to progressive loss of renal function. The first abnormal study was performed before the initiation of therapy in November when there was marked reduction of the left urine flow fraction (to 8%) and a less striking reduction in left perfusion fraction (23%). An arteriogram performed shortly thereafter showed a probably significant stenosis of the left main renal artery. Other medical complications forced the use of conservative therapy, and the patient's course was followed with additional studies. The studies from January through May show a progressive loss in left ERPF and reduction in left urine flow fraction. The TCCC fell for both the in-

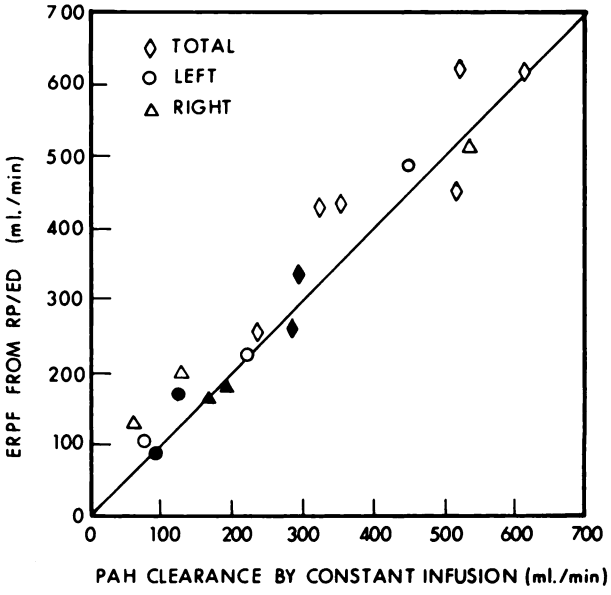

FIG. 5. Comparisons of total ERPF obtained by RP/ED and constant-infusion split-function tests. Diagonal line is identity for reference. Darkened symbols represent cases of surgically proven unilateral main renal artery disease.

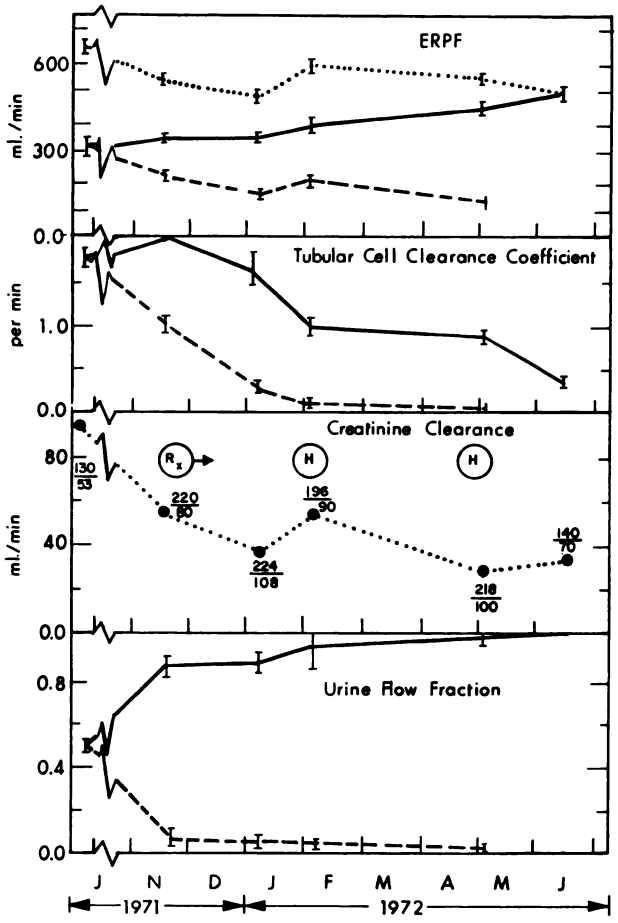

FIG. 6. RP/ED series showing progressive loss of renal function in Patient AM with proven left main renal artery stenosis. Left nephrectomy was performed in June 1972; hence only right kidney data are available thereafter. Antihypertensive medication is represented by R_x and retinal hemorrhages by H. (- - - - left, —— right, ... total).

volved and uninvolved kidneys (left TCCC from 0.13 to 0.07/min and right TCCC from 1.6 to 0.86/min). This fall was coincident with a reduction in creatinine clearance from 58 to 26 ml/min.

Acute renal failure. Often it is not possible to perform an arteriogram or an IVP in the oliguric or anuric patient. We have found that the RP/ED is helpful in such cases. Three examples are presented.

Renal vein thrombosis: Fig. 7 shows serial studies of a patient (MC) who had a surgically proven diagnosis of inferior vena caval and bilateral renal vein thrombosis. At the time of the first radiohippurate study, she had been anuric and was maintained on renal dialysis for a period of 9 days. Accordingly, neither an IVP nor arteriogram were possible; hence, it was not known if there were any functioning renal parenchyma. The first RP/ED indicated that ERPF was 219 ml/min. Some recovery was predicted since an ERPF of this magnitude has been associated with production of urine. Two days later the patient began to pass urine, and a dramatic clinical improvement ensued. By the third RP/ED study, ERPF was normal (696 ml/min). An arteriogram performed immediately thereafter showed mild bilateral fibromuscular hyperplasia and no other abnormalities. Serial scintiphotos performed in the OIH studies showed significant accumulation of hippurate in the kidneys but it was impossible to determine the course and degree of therapeutic response of renal function from the pictures alone. Also of interest was the relative increase of function for the left kidney as the patient improved. The cause of this is uncertain; however, a large avascular mass displacing the right kidney was apparent on both the IVP and renal scintiphotos.

Urinary obstruction: serial studies before and after passage of a ureteral stone are presented in Fig. 8. This patient (NG) experienced sudden onset of renal colic and had abundant microscopic hematuria 12 hr before the first RP/ED. This test is interesting because it demonstrates the degree to which

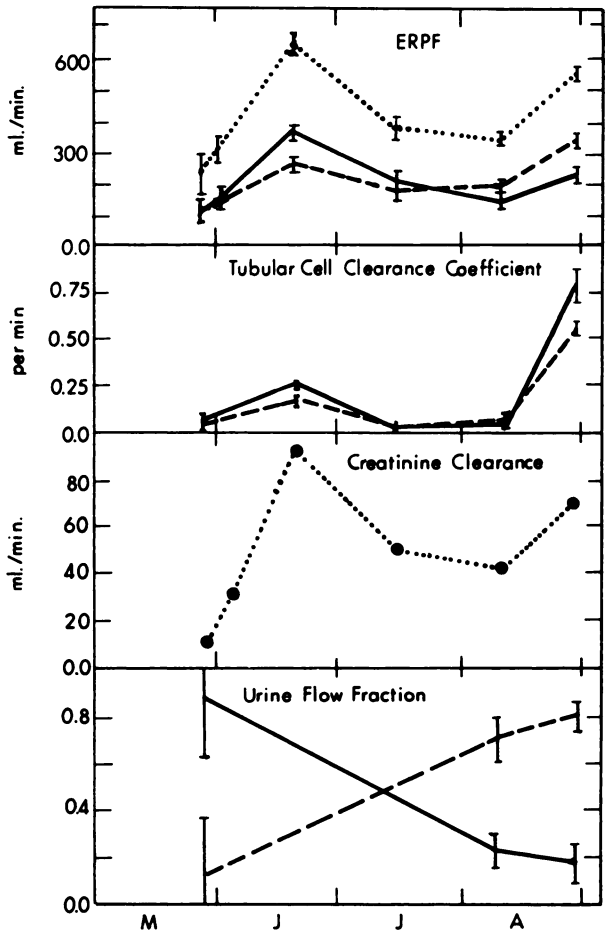

FIG. 7. RP/ED series showing recovery of renal function in Patient MC with inferior vena caval and bilateral renal vein occlusion (- - - - left, —— right, ... total).

blood flow can be separated from urine outflow. The ERPF for the left kidney was normal (325 ml/min), while the TCCC, TTT, and urine flow fractions were strikingly abnormal (TCCC less than 0.02, TTT greater than 18 min, urine flow fraction less than 8%). All measurements were normal for the right kidney. Subsequent tests showed stepwise return of the abnormal parameters to normal (last TCCC was 0.37 per min, TTT was 1.3 min, urine flow fraction was 35%) coincident with passage of the stone and subsidence of symptoms.

Transplantations: fourteen patients have been followed with serial studies to determine the possible use of the RP/ED for the determination of transplant rejection, acute tubular necrosis, and for the evaluation of the therapeutic response. Of these, 11 patients experienced a clinical syndrome of transplant rejection within the first 3 months. Histologic confirmation of this diagnosis was obtained in nine cases. The RP/ED results obtained at the time of early rejection were characterized by a modest reduction of RPC to 0.9 ± 0.2 of its prerejection value a sharp drop in TCCC to 0.3 ± 0.2 of its prerejection value (usually the first sign of rejection), and little change in TTT unless the rejection process was far advanced.

Serial studies on one patient (DA) are presented in Fig. 9. The initial RP/ED was done on the first postoperative day because the patient had experienced a period of hypotension. Renal perfusion was low though adequate (RPC = 0.084 per min, as seen with acute tubular necrosis, and the excretory parameters were normal (TCCC = 0.20 per min, TTT = 1.5 min). Four days post-transplant the RPC had risen to 0.20 and on Day 6 to 0.37. TCCC fell precipitously from 0.23 on Day 4 to an abnormally low value of 0.06 on Day 6. No abnormalities of TTT were noted, however. Based on these findings, diagnosis of acute transplant rejection was made. The patient was clinically stable although she was hypertensive and had a streptococcal wound infection. The RP/ED was repeated on Day 6 and the findings confirmed. Appropriate additional therapy was initiated. On Day 12 the RPC had declined to 0.235 and the creatinine clearance had declined to 34 ml/min from 45 ml/min. These findings were interpreted as indicating progression of rejection in spite of additional therapy. By Day 15, the RPC had fallen to 0.04 and the TCCC was 0.35. The reduced RPC indicated very little effective perfusion although some nephrons (presumably medullary) did have relatively good function. Severe cortical necrosis was predicted from the low value of RPC and was confirmed by open renal biopsy the next day. Subsequently, the RPC rose to 0.14 on Day 18

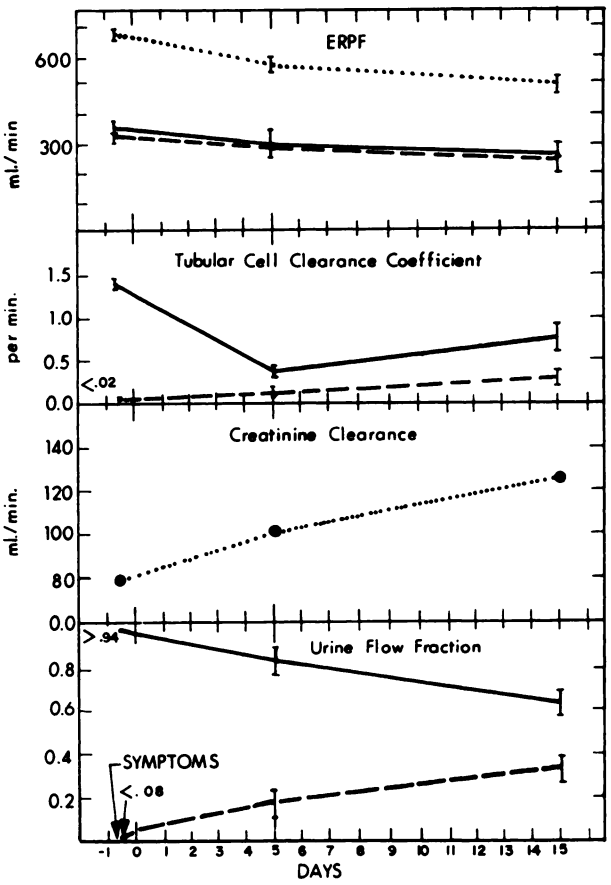

FIG. 8. RP/ED series in Patient NG before and after (Day 0) passage of left renal stone. (- - - - left, —— right, ... total).

although the patient was anuric, and was 0.11 on Day 22 when the patient was passing approximately 0.6 liters of urine per day. Initial recovery from transplant rejection was indicated by the increased RPC on Day 18. Unfortunately, persistent wound infection forced removal of the kidney. Pathologic examination showed healing of the rejection process with no active necrosis.

DISCUSSION

Qualitative observations of the clearance of OIH from the kidney do not permit quantitative statements about renal physiology unless there is an abnormality such as complete loss of blood supply or a complete obstruction to urine flow. Quantitative clinical estimates of renal function are possible, however, by the application of parameter estimation techniques to multicompartmental models of renal physiology, yielding information not obtainable from the conventional renogram. This includes quantitative determination of total and unilateral ERPF, the rate of accumulation and clearance of isotope from the kidney tubules, and the time of transit of isotope in urine through the collecting system into the bladder. The gamma camera scintiphotos are an integral

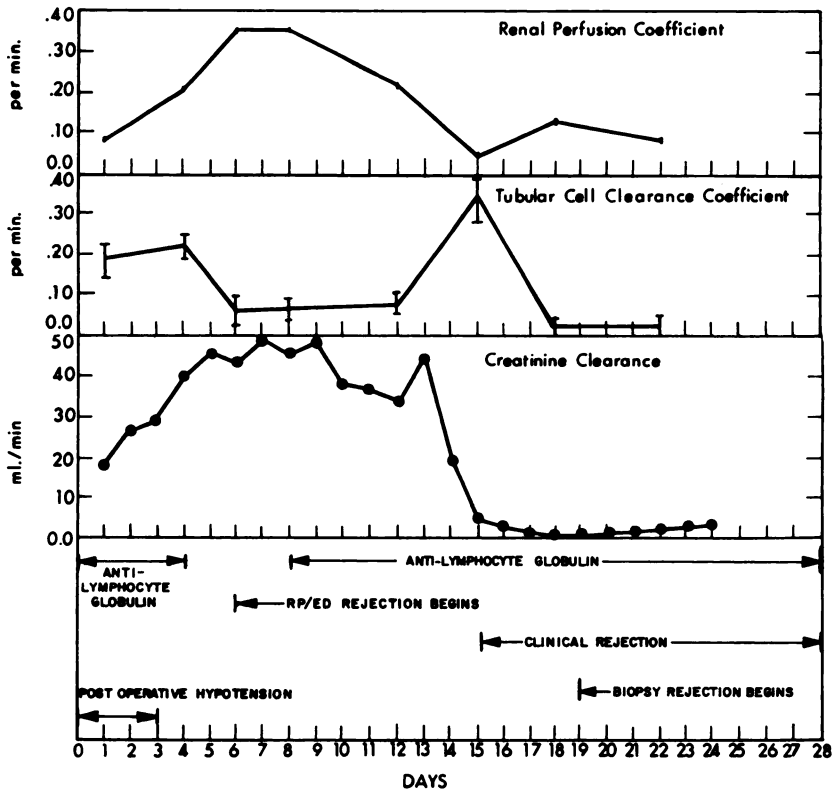

FIG. 9. Transplant rejection (Patient DA). Serial studies began immediately postsurgery (Day 1). RP/ED indicates rejection on Day 6.

part of the test and RP/ED report; the photos give important, although gross, detail about renal size, the presence of ureteral dilation, and the location of an obstruction and/or fistula.

The RP/ED is thus a renal split-function test which has many similarities to constant-infusion tests with PAH and inulin but does not suffer many of its procedural disadvantages. The latter requires approximately 3 hr of operating-room time since both ureteral catheterization and saddle anesthesia are used. Additional hours or days are needed for patient observation after the removal of the ureteral catheters. Consequently, the test cannot be done on an outpatient basis and it has never gained broad application (*43*). One important difference between these tests is that the RP/ED does not determine GFR. This could be overcome by the addition of a second isotope, such as iothalamate, to the study.

Several other models of the physiology of OIH clearance from the body have been reported (*10–14*). To our knowledge, all of these are distinctly different from the present work and none can be so completely related to split-function renal studies. For example, Comyn, et al (*10*) have not used a gamma camera probe system and they do not explicitly describe the exchanges of OIH in other than kidney pools. The work of Meldolesi, et al (*11*) does not model the exchange of extra-renal distribution of isotope. Comyn, Horgan, and Knudsen (*10,12,13*) use model simulation only. Meldolesi (*11*) and Heiskanen (*14*) either do not provide an error analysis of the observational data or do not describe the parameter estimation techniques they use.

Although our normal series is still small, the data do support the hypothesis that approximately the same normal ranges apply to both the split-function test and the RP/ED. Our studies show that in a series of normal patients there is a rather broad range of individual parameters; similar variation has been observed in studies with constant-infusion techniques (*34,36,44,45*). The full significance of these variations is not known although it is clear that the patient's state of hydration must be regulated within the suggested boundaries to optimize urine flow rates and RP/ED results. As in the constant-infusion test, however, the high degree of individual variation is often unimportant since even greater differences are seen in renal diseases.

The pathological cases presented suggest that this new test has broad clinical application. When applied to the study of patients with unilateral renal artery stenosis, observed values of renal perfusion and urine flow fraction are reduced ipsilaterally as expected. These findings are analogous to those obtained in constant-infusion testing of similar or the same patients; the findings reflect reduced tubular cell function and increased water reabsorption by the affected kidney (*17*). Patients with essential hypertension,

who do not have advanced renal demage, do not have similar asymmetrical abnormalities. When renal damage is severe, however, the RPC, ERPF, and TCCC may be significantly reduced for both kidneys; the urine flow fractions, on the other hand, will usually be consistent with estimates of relative renal size and will usually be within the normal range (*32*).

A major use for this test should be the determination of the contribution of each kidney to total renal function (*32*). While it is true that the RP/ED often correlates well with the results of arteriography, we have encountered instances (not presented) where this is not the case. For example, severe unilateral renal disease has been overlooked because the arteriogram only showed renal artery stenosis of the opposite kidney (RP/ED and Stamey tests were normal for this kidney). Remarkably, the split-function test and RP/ED both showed severe disease of the arteriographically normal kidney. This information was of extreme importance for the surgeon who had to choose between ablative, reconstructive, or no surgery for correction of the renal artery stenosis.

Estimates of renal function were also possible in oliguric or anuric patients when GFR was too low to permit sufficient concentration of contrast material used in the usual x-ray procedures. The studies of transplant rejection are a most interesting example of this. OIH extraction is not GFR dependent and will concentrate in the kidney as long as there is plasma flow and proximal tubular cell function. The cases presented illustrate these applications. The first sign of rejection appears to be a reduction in the TCCC. We have seen this change precede (by several days) changes in other tests, such as creatinine clearance and tests of cellular-immunocompetence. ERPF may actually rise when the TCCC clearly indicates that rejection is probable. We recognize that reduced cortical perfusion is an early finding in rejection (*46*), and we are puzzled that an earlier effect on tubular cell accumulation of OIH is not observed. Perhaps this is related to the redistribution of blood flow that precedes a reduction of total flow in such cases (*47*). Ultimately, ERPF is reduced and it indicates extensive damage to the kidney. Also, an increase in ERPF is the first indication of recovery while the TCCC is rather slow to respond.

Finally, it is estimated that the radiation exposure from a single RP/ED is approximately 300 mrads to the kidney, 6 mrads to the bladder and ureter, 120 mrads to the thyroid, and 90 mrads to the whole body (*48–50*). Thus, there is a small but very real radiation hazard associated with these tests. In serial studies one must weigh the risks against the potential value of the data obtained. Where the test is used to determine the dose of an immunosuppressive agent or the timing of a surgical procedure, we feel that the relative hazard of the test is small.

In conclusion, we have presented a series of cases that illustrate our experience with the use of the RP/ED for the clinical evaluation of renal function. Our results indicate that the information provided will be useful for the evaluation of therapeutic response and for the diagnosis of a number of disorders of the kidney. Serial studies indicate that in some well-defined cases, the test may also permit a prediction of the patient's course. It is our belief that these studies demonstrate the potential value of this relatively new approach in which a large computer is used in the interpretation of nuclear medicine procedures, and that they are useful models for the development of other tests using different radionuclides. We believe that additional investigative effort in this direction is clearly justified by the data presented.

ACKNOWLEDGMENTS

Special thanks are due David Feller of NASA, Ames, for his kind support of part of this work and to Allan Twarowski and Michael McClury for their technical assistance in the development of the methods used. We are also indebted to other workers and institutions for making available to us the results of split-function studies.

This work was supported in part by a James Picker Foundation (National Academy of Science) Grant, Stanford University Grant FR-05353-07, Grant NGR578 of the National Aeronautics and Space Administration, PHS-FHPS Grant SF(Y)73-8-63, and by Analytical Development Associates Corporation, Cupertino, Calif.

APPENDIX: MATHEMATICAL MODEL SUMMARY

A mathematical model of the renovascular system which includes just the pathways for OIH clearance is summarized here. This model is composed of:

1. A dynamic flow model describing the OIH distribution and clearance in body compartments.
2. An observational model that relates the dynamic flow model to the observations made by the scintillation detectors, and
3. A statistical model of the counting errors.

The model is summarized here.

Mathematical description of the hydraulic model. The following conservation equations describe the flows depicted in Fig. 2. The net rate of change, $\dot{q}$, of quantity of OIH, q_1, in Compartment 1 at any time (t) is

$$\dot{q}_1(t) = -(\alpha_1 + \alpha_4)q_1(t) + \alpha_5 q_5(t)$$

$$\text{with } q_1(0) = (1 - f_1 - f_2)A \quad (1)$$

where A is the total radioactivity injected and f_1 and f_2 are the fractions of isotope deposited in the kidneys and Compartment 5 at the beginning of the

modeling operation. A negative sign preceding a term indicates an outflow rate.

The right tubular cell compartment has

$$\dot{q}_2(t) = (1-\beta)\alpha_1 q_1(t) - \alpha_2 q_2(t) \quad \text{with } q_2(0) = (1-\beta) f_1 A. \quad (2)$$

A fraction $(1-\beta)$ of the total effective renal flow appears as input to the right kidney. Similarly, the left proximal tubular cell compartment has

$$\dot{q}_3(t) = \beta\alpha_1 q_1(t) - \alpha_3 q_3(t) \text{ with } q_3(0) = \beta f_1 A \quad (3)$$

since the remaining fraction, β, of the total effective renal flow is input to the left kidney. The rate of change of OIH in the bladder is

$$\dot{q}_4(t) = \alpha_2 q_2(t-\tau_2) + \alpha_3 q_3(t-\tau_1) \quad \text{with } q_4(0) = 0. \quad (4)$$

The inflow to the bladder is the outflow from each kidney's tubular cell compartment delayed by the transport time along the tubules. No outflow from the bladder is assumed to occur over the course of the examination. If bladder catheterization is present, the bladder detector is not used and the observation relations are appropriately modified.

Compartment 5 has

$$\dot{q}_5(t) = \alpha_4 q_1(t) - \alpha_5 q_5(t) \text{ with } q_5(0) = f_2 A. \quad (5)$$

Compartment τ_1 has an inflow of $\alpha_3 q_3(t)$ and an outflow of $\alpha_3 q_3(t-\tau_1)$ at a time, t; hence

$$\dot{q}_{\tau_1}(t) = \alpha_3[q_3(t) - q_3(t-\tau_1)] \quad \text{with } q_{\tau_1}(t) = 0 \text{ for } -\tau_1 \leq t \leq 0; \quad (6)$$

the value of $q_{\tau_1}(t)$ is the quantity of OIH present in compartment τ_1 at a time, t. Similarly,

$$\dot{q}_{\tau_2}(t) = \alpha_2[q_2(t) - q_2(t-\tau_2)] \quad \text{with } q_{\tau_2}(t) = 0 \text{ for } -\tau_2 \leq t \leq 0 \quad (7)$$

for Compartment τ_2.

The gamma detector positioned over the left kidney would observe

$$\hat{r}_1(t) = \gamma_1[q_1(t) + q_5(t)] + \gamma_3 q_4(t) + q_3(t) + q_{\tau_1}(t) \quad (8)$$

if background and gamma camera split-field cross-coupling were neglected. In Eq. 8 the radioactivity observed by the detector is given unity coefficient for the kidney contribution, $q_3 + q_{\tau_1}$ while the extra-renal contribution is $\gamma_1(q_1 + q_5)$ where γ_1 is the observation fraction of the extra-renal compartments. Similarly, $\gamma_3 q_4$ is the contribution of scattering or direct view of the bladder compartment with γ_3 the fraction of the bladder compartment observed by the left kidney detector.

In the same manner one obtains

$$\hat{r}_2(t) = \gamma_2[q_1(t) + q_5(t)] + \gamma_4 q_4(t) + q_2(t) + q_{\tau_2}(t), \quad (9)$$

$$\hat{r}_3(t) = \gamma_5[q_1(t) + q_5(t)] + \gamma_6[q_3(t) + q_{\tau_1}(t)] + \gamma_7[q_2(t) + q_{\tau_2}(t)] + \gamma_8 q_4(t), \quad (10)$$

$$\hat{r}_4(t) = \gamma_9[q_1(t) + q_5(t)] + \gamma_{10}[q_3(t) + q_{\tau_1}(t)] + \gamma_{11}[q_2(t) + q_{\tau_2}(t)] + \gamma_{12} q_4(t) \quad (11)$$

for the observations without cross-coupling or background for the right kidney, bladder, and precordial gamma detectors, respectively. The γ_i are the observation fractions (of the quantities on which they appear as multipliers) associated with the observations on the left of the equations. The expected observations from gamma detectors over left kidney, right kidney, bladder and precordium, respectively, including backgrounds and cross-coupling, are then

$$r_1(t) = \hat{r}_1(t) + \delta_{12}\hat{r}_2(t) + b_1 \quad (12)$$

$$r_2(t) = \delta_{21}\hat{r}_1(t) + \hat{r}_2(t) + b_2 \quad (13)$$

$$r_3(t) = \hat{r}_3(t) + b_3 \quad (14)$$

$$r_4(t) = \hat{r}_4(t) + b_4 \quad (15)$$

where δ_{12} is the cross-coupling coefficient (usually measured at the end of the test procedure) from right to left, δ_{21} is the cross-coupling coefficient measured from left to right, and the b_i are background counting rates with the subject in position.

Certain of the observation fractions, the γ_i, in Eqs. 8–11 may be known to be zero; for example, γ_{12} is typically zero since the bladder is usually not viewed by the precordial gamma detector.

Parameter estimation and error propagation. The mathematical model of the dynamic system and observations as outlined in the previous section includes a number of unknown parameters pertinent to each individual subject. These include α_1 to α_5, β, f_1, f_2, τ_1, τ_2, and A of Eqs. 1–7; also included are a large subset of the γ_i of Eqs. 8–11. These unknown parameters are denoted by a parameter vector, p, for convenience in what follows.

Suppose K data sets (typically, $K = 4$) are available; the k-th data set has M_k data points. The time of occurrence of the m-th point from the k-th set with the value ρ_{mk} is t_{mk}. The calculated value of the observation is $r_k(t_{mk})$ as given in the previous section. An iterative technique (a modified Gauss-Newton iteration) is used to obtain estimates of the N elements of the parameter vector, p. At the i-th iteration, the difference between the observed and calculated data is

$$\phi^i_{mk} = \rho_{mk} - r^i_k(t_{mk}) \qquad (16)$$

with parameter vector p^i. Also, at the i-th iteration, let

$$\frac{\partial r^i_k(t_{mk})}{\partial p_l}$$

evaluated with $p = p^i$, be the (m,l) element of the matrix A^i_k. The evaluation of the elements requires the use of the chain rule and the observational equation relating the states and observables as well as the evaluation of the partial derivatives

$$\frac{\partial q_i}{\partial p_j}$$

at each time point of interest and each iteration. The inverse of the covariance matrix of the observational errors is W_k with elements w_{ijk} for the k-th data set and the errors in each data set assumed independent. The error at the i-th iteration is then

$$\epsilon^i = \sum_{k=1}^{K} \sum_{m=1}^{M_k} \sum_{n=1}^{M_k} \phi^i_{mk} W_{mnk} \phi^i_{nk}. \qquad (17)$$

The Gauss-Newton iteration scheme (*31*) then states that

$$\left[\sum_{k=1}^{K} A^i_k W_k A^i_k\right](p^{i+1} - p^i) = \left[\sum_{k=1}^{K}\right] A^{i\prime}_k W_k \phi^i_k \qquad (18)$$

where ϕ^i_k is the residual vector for the i-th iteration and the k-th data set, i.e., the vector with elements ϕ^i_{mk}, $m = 1, 2, \ldots, M_k$; the superscript: denotes transpose. A modification of Eq. 18 useful in convergence control is

$$\left[\left(\sum_{k=1}^{K} A^{i\prime}_k W_k A^i_k\right) + \lambda D^i\right](p^{i+1} - p^i) = \left[\sum_{K=1}^{K} A^{i\prime}_k W_k \phi^i_k\right] \qquad (19)$$

where D^i is the diagonal part of the sum in the brackets on the left of Eq. 18 and λ is chosen to appropriately bound the parameter changes. Equation 19 is solved at each iteration to obtain p^{i+1} which is then used to obtain $A_k{}^{i+1}$ and the $\phi_k{}^{i+1}$ for the next iteration. The initial parameter vector, p^0, is an input to the iterative procedure. Since the underlying data noise is Poisson distributed and usually independent from observation to observation, W_k is a diagonal matrix with elements $w_{mmk} = 1/\lambda_{mk}$ where λ_{mk} is the mean (and also variance) of the process. In practice, the λ_{mk} are replaced by an estimate of the mean obtained directly from the data. The estimated parameters obtained by the above procedure have a covariance matrix for small deviations given by the inverse of the matrix in brackets to the left of the equal sign in Eq. 18. This covariance matrix is nearly the smallest possible (*31*). The square root of the diagonal elements of the covariance matrix (standard error of the parameter determinations) is made available on the clinical report. A subset of the matrix is used to calculate the standard errors presented in the "Derived Results" section of the RP/ED output form. Further, goodness-of-fit tests are applied to the error ϵ^i existing at the final iteration to judge the correctness of the dynamic model and observational relations.

REFERENCES

1. TAPLIN GV, MEREDITH OM, KADE H, et al: The radioisotope renogram. *J Lab Clin Med* 48: 886–956, 1956
2. NORDYKE RA, GILBERT FI JR, SIMMONS EL: Screening for kidney disease with radioisotopes. *JAMA* 208: 493–496, 1969
3. MAXWELL MH, LUPU AN, TAPLIN GV: Radioisotope renogram in renal arterial hypertension. *J Urol* 100: 376–383, 1968
4. MANI P, JOHNSON PC, SCOTT R, et al: A comparison of renogram curves before and after renovascular reconstructive surgery for hypertension. *J Urol* 101: 16–20, 1969
5. BRITTON KE, BROWN NJG: *Clinical Renography*, Chicago, Yearbook Medical Publishers, 1971
6. WITCOFSKI RL, WHITLEY JE, MESCHAN I, et al: A method and parameters for the analysis of renal function by external scintillation detector technic. *Radiology* 76: 621–625, 1961
7. MEADE RC, HORGAN JD, MADDEN JA: Comparison of methods for renogram evaluation. *J Nucl Med* 10: 40–45, 1969
8. BROWN NJG, BRITTON KE: A new system of renography. *Biomed Eng* 4: 268–274, 1969
9. HOLROYD AM, CHISHOLM GD, GLASS HI: The quantitative analysis of renograms using the gamma camera. *Phys Med Biol* 15: 483–492, 1970
10. COMYN G, LESIEUR J, PARMENTIER P, et al: Le nephrogramme isotopique (modele analogique exploite sur ordinateur). *J d'Inform Med Toulouse*, March, 1969
11. MELDOLESI U, RONCARI G, FIDANZA MA, et al: First attempts of clinical application of a method for the quantitative interpretation of renogram with radiohippuran. *J Nucl Biol Med* 13: 94–102, 1969
12. HORGAN JD, MEADE RC, MADDEN JA, et al: Digital computer simulation study of the radiohippuran renogram. *Int J Appl Radiat Isot* 18: 797–805, 1967
13. KNUDSEN E, SØE HØJBERG K: Simulation of the radiohippuran renogram test on an analogue computer. *Int J Appl Radiat Isot* 18: 639–646, 1967
14. HEISKANEN T, WEBER T, GRASBECK R: A model for the quantitative evaluation of radioisotope renograms. *Int J Appl Radiat Isot* 19: 827–834, 1968
15. JACKSON PE, SCHEIBE PO: Computer-aided renogram interpretation. *Conf Rec 3rd Asilomar Conf Circuits and Systems*, North Hollywood, Western Periodicals, 1969, pp 20–28
16. BELL WR, JACKSON PE, MEYER ER, et al: A simulation of the renal perfusion and excretory system. *Proc Sum-*

mer Computer Simulation Conf, Denver, ACM/SHARE/SCi, 1970, pp 913–920

17. STAMEY TA, NUDELMAN IJ, GOOD PH, et al: Functional characteristics of renovascular hypertension. *Medicine* 40: 347–392, 1961

18. MAGNUSSON GA: Kidney function studies with ^{131}I-tagged sodium orthohippurate. *Acta Med Scand* [*Suppl*] 171: 94–124, 1962

19. SMITH HW: *Principles of Renal Physiology.* New York, Oxford Univ Press, 1956, pp 57, 62, 64

20. BURBANK MK, TAUXE WN, MAHER FT, et al: Evaluation of radioiodinated hippuran for the estimation of renal plasma flow. *Staff Meet Mayo Clin* 36: 372–386, 1961

21. TAUXE WN, MAHER FT, TAYLOR WF: Effective renal plasma flow: estimation from theoretical volumes of distribution of intravenously injected ^{131}I orthoiodohippurate. *Mayo Clin Proc* 46: 524–531, 1971

22. MAGNUSSON GA: Kidney function studies with ^{131}I-tagged sodium orothoiodohippurate. *Acta Med Scand* [*Suppl*] 171: 7–31, 1962

23. GUYTON AC: *Textbook of Medical Physiology.* Philadelphia, WB Saunders, 1968, pp 435–436

24. WEDEEN RP: Autoradiography of hippuran-I^{125} in rat kidney; the intrarenal basis of the radioisotope renogram. *Radioisotopes in the Diagnosis of Diseases of the Kidneys and the Urinary Tract,* Timmermans L, Merchie G, eds, Amsterdam, Exerpta Medica Foundation, 1969, pp 461–466

25. SMITH HW: *Principles of Renal Physiology,* New York, Oxford Univ Press, 1956, pp 55–60

26. PITTS RF: *Physiology of the Kidney and Body Fluids,* Chicago, Year Book Medical Publishers, 1963, pp 129–135

27. PITTS RF: *Physiology of the Kidney and Body Fluids,* Chicago, Year Book Medical Publishers, 1963, pp 130–131

28. SCHEIBE PO, JACKSON PE: A physio-mathematical model of OIH dynamics. In preparation

29. FARMELANT MH, SACHS CE, GENNA S, et al: A physiological model for the renal excretion of labeled compounds. *J Nucl Med* 10: 664–671, 1969

30. FARMELANT MH, BAKOS K, BURROWS BA: Physiological determinants of renal tubular passage times. *J Nucl Med* 10: 641–645, 1969

31. DEUTSCH R: *Estimation Theory,* Englewood Cliffs, NJ, Prentice-Hall, 1965, pp 60–66

32. STAMEY TA: *Renovascular Hypertension,* Baltimore, Williams and Wilkins, 1963

33. SMITH HW: *Principles of Renal Physiology,* New York, Oxford Univ Press, 1956, p 58

34. SMITH HW: *Principles of Renal Physiology,* New York, Oxford Univ Press, 1956, pp 32, 89

35. SMITH HW: *The Kidney, Structure and Function in Health and Disease,* New York, Oxford Univ Press, 1951, pp 296, 543

36. STAMEY TA: *Renovascular Hypertension,* Baltimore, Williams and Wilkins, 1963, pp 88–89

37. FAIR WR, STAMEY TA: Differential renal function studies in segmental renal ischemia. *JAMA* 217: 790–793, 1971

38. FAIR WR: Difficulties in the evaluation of hypertension secondary to renal ischemia. *Urologia Internationalis* 25: 393–414, 1970

39. PITTS RF: *Physiology of the Kidney and Body Fluids,* Chicago, Year Book Medical Publishers, 1963, pp 15–20

40. GUYTON AC: *Textbook of Medical Physiology,* Philadelphia, WB Saunders, 1968, p 478

41. SMITH HW: *Principles of Renal Physiology,* New York, Oxford Univ Press, 1956, pp 65–67

42. STAMEY TA: *Renovascular Hypertension,* Baltimore, Williams and Wilkins, 1963, pp 212–217

43. STAMEY TA: Measurement of renal vein renins or differential renal function studies in the diagnosis of curable renovascular hypertension? *Urological Research,* Plenum Press, 1972, pp 131–148

44. SIMON NM, DEL GRECO F. O'CONNOR VJ: Differential renal function studies during mannitol diuresis in hypertension. *Circulation* 33: 789–795, 1966

45. MAXWELL MH, LUPU AN, KAUFMAN JJ: Individual kidney function tests in renal arterial hypertension. *J Urol* 100: 384–394, 1968

46. KOUNTZ S, LAUB DR, COHN R: Detecting and treating early renal homotransplant rejection. *JAMA* 191: No. 12, 997–1001, 1965

47. HOLLENBERG NK, EPSTEIN M, ROSEN SM, et al: Acute oliguric renal failure in man: evidence for preferential renal cortical ischemia. *Medicine* 47: 455–474, 1968

48. CHANTRAINE JM: Radiation hazard associated with renal investigations using radioisotopes. *Radioisotopes in the Diagnosis of Diseases of the Kidneys and Urinary Tract,* Timmermans L, Merchie G, eds, Amsterdam, Exerpta Medica Foundation, 1969, pp 627–630

49. NORDYKE RA, TUBIS M, BLAHD WH: Use of radioiodinated hippuran for individual kidney function tests. *J Lab Clin Med* 56: 438–445, 1960

50. SELTZER RA, KEREIAKES JG, SAENGER EL, et al: Radiation exposure from radioiodine compounds in pediatrics. *Radiology* 82: 486–494, 1964